Co-published by
Institute of Fluid-Flow Machinery
Polish Academy of Sciences
Committee on Thermodynamics and Combustion
Polish Academy of Sciences

http://www.imp.gda.pl/archives-of-thermodynamics/

ARCHIVES OF THERMODYNAMICS

Experimental and statistical determination of thermal characteristics of the special design minichannel heat exchanger

Maria Karolina Tychanicz-Kwiecień[a*], Witold Rajmund Rybiński[b]

[a]Rzeszow University of Technology, al. Powstańców Warszawy 12, 35-959 Rzeszów, Poland
[b]Institute of Fluid Flow Machinery, Polish Academy of Science, ul. Fiszera 14, 80-231 Gdańsk, Poland
*Corresponding author email: mtychanicz@prz.edu.pl

Received: 28.12.2023; revised: 28.02.2024; accepted: 25.03.2024

Abstract

The paper presents the results of experimental investigation and the new statistical method for the determination of preliminary thermal characteristics of a prototype compact minichannel heat exchanger with laminar flows and significant heat transfer in the manifolds. The exemplary heat exchanger consists of 9 straight, parallel, square-shaped channels and two rectangular-shaped manifolds milled on both sides of the single aluminium plate. The design of the investigated heat exchanger is quite particular, as the heat transfer area of both pairs of manifolds provides almost 1/3 of the total heat transfer area. In the new statistical method presented in this paper, the manifolds' and channels' heat flows are considered separately. The heat exchanger's thermal characteristic was obtained statistically on the basis of the experimental results and is presented in the form of the overall heat transfer rate. The developed thermal characteristic model accounts for two effects, among many others, which may affect heat transfer in the exchanger, i.e. the heat loss to the ambient and the significant heat transfer in the manifolds. It is proved that the heat transfer to the surroundings was negligible due to the suitable thermal insulation. In order to demonstrate that the heat transfer in the manifolds is significant, two calculation variants are presented. The relative differences (residuals) between the experimental and statistically corrected heat transfer rates and the coefficient of determination R^2 are determined in both variants. In the first variant the heat transfer in the manifold pairs is neglected and in the second model it is included. It was observed that the lack of consideration of the heat transfer in the manifold pairs provides drastic dispersion between the experimental and statistical results. In turn, in the second model, where the manifolds are accounted for, a significant enhancement in the consistency of the results is noticed. The relative residuals are much lower, and the corresponding coefficient R^2 is improved from $R^2 = 0.8827$ in the first variant to $R^2 = 0.9335$ in the second one, respectively.

Keywords: Minichannel heat exchanger; Statistical analysis; Thermal characteristics; Laminar flows; Wilson plot

Vol. 45(2024), No. 2, 63–71; doi: 10.24425/ather.2024.150852

Cite this manuscript as: Tychanicz-Kwiecień, M.K., & Rybiński, W.R. (2024). Experimental and statistical determination of thermal characteristics of the special design minichannel heat exchanger. *Archives of Thermodynamics*, 45(2), 63–71.

1. Introduction

For the last decades the revolutionary development of compact miniature systems and installations, particularly for heating and cooling applications and increasing demands in terms of rational thermal energy management, have led to the decrease in size of heat transfer equipment. Heat exchangers of small hydraulic diameter, also called minichannel heat exchangers have received much attention so far due to meeting the requirement of transferring high heat flux rates in small volume and providing thermal performance augmentation. In the view of compact design

Nomenclature

A – heat transfer area, m^2
a – channels or manifolds width, m
b – channels or manifolds height, m
c – correction coefficient
c_p – specific heat capacity at constant pressure, J/(kg·K)
d – wall thickness, m
d_h – hydraulic diameter, m
h – specific enthalpy, J/kg
k – overall heat transfer coefficient, W/(m^2·K)
L – channels or manifolds length, m
N – number of measurements
n – number of channels
Nu – Nusselt number
Pr – Prandtl number
p – pressure, Pa
$\dot{Q}$ – heat flow rate, W
Re – Reynolds number
r_{ba} – normalized aspect ratio
res_{rel} – relative residual
S – cross-sectional area, m^2
T – temperature, K
$\dot{V}$ – volumetric flow rate, m^3/s
W – heat capacity rate, W/K

Greek symbols

α – heat transfer coefficient, W/(m^2·K)
ΔT_{log} – logarithmic mean temperature difference, K
λ – thermal conductivity, W/(m·K)
μ – dynamic viscosity, Pa·s
ρ – density, kg/m^3
φ – sum of squares, 1/W^2

Subscripts and Superscripts

3 – 3-sided channel
4 – 4-sided channel
A – manifold pair A
B – manifold pair B
c – cold
h – hot
chn – channel
mf – manifold
exp – experimental
$pred$ – predicted
$corr$ – corrected
fd – fully developed flow
in – inlet
out – outlet
lam – laminar
$turb$ – turbulent
rel – relative

and accompanying size reduction of minichannel heat exchangers, the analysis of heat transfer and fluid flow have gained particular attention and became a developing research area.

Accurate thermal and flow performance characterization for prescribed mini- and microchannel system require the consideration of scaling effects [1, 2], design concerns, like the shape and geometry of channels and manifolds [3] as well as flow development and boundary conditions.

In minichannel heat exchangers with two single-phase fluid flows, the determination of thermal characteristics is rather complex as heat transfer generally covers not only the channel region, but often also the inlet and outlet manifolds and additional effects are more feasible to occur. A common approach to estimate thermal characteristics for a given minichannel system is to use simplified analytical heat transfer prediction models and literature correlations appropriate for conventional-size channels. However, it is frequently observed that results obtained are questionable and sometimes inconsistent with theoretical predictions as the fact that assumed boundary conditions are not exactly fulfilled or additional phenomena may occur that were not accounted in the simplified model [4, 5]. The literature survey concerning mini- and microchannel heat exchangers revealed that the studies are rather focused on their practical applications with the aim of presenting overall thermal and hydraulic performance evaluation and effectiveness of the entire heat exchanger, what was reported in following exemplary papers [6–14]. The authors also investigated the optimization of mini- and microchannel heat exchangers design in terms of thermal and hydraulic performance improvement [15]. The consistency of obtained experimental thermal characteristics of mini- and microchannel heat exchangers with fundamental theories of heat transfer and fluid flow in ducts was studied as well [16].

Experimental determination of heat transfer coefficient for particular minichannel heat exchanger requires careful determination of the surface temperature and surrounding fluid. However, accurate experimental measurements of the temperature inside mini-heat exchanger channels in particular are extremely difficult or are even impossible in practice. In order to overcome the temperature measurement impediments, statistical determination of thermal characteristics for minichannel heat exchangers can be considered. Statistical methods, based on the Wilson plot method, use external experimental measurements of heat exchanger's parameters and enable detailed analysis of thermal behavior of investigated heat exchanger [17]. Fernando et al. [18] obtained heat transfer coefficients for shell-and-tube heat exchanger with multiport minichannel tubes with the use of classical version of the Wilson plot method. The comparison of obtained results of Nusselt number and heat transfer coefficients with standard literature correlations reflected partial, but no clear correspondence, especially in the laminar flow regime. In [19] new statistical method was derived for the determination of thermal characteristic of a prototype heat exchanger made of two plates with mini channels. The obtained experimental thermal characteristics of investigated heat exchanger were given in the form of overall thermal resistance. Since the experimental and theoretical thermal resistances are predominantly not equal, corrected thermal resistance was introduced to statistically estimate experimental thermal resistance. The regression function of corrected overall thermal resistance included two experimental linear coefficients, which corrected the predicted thermal resistance of hot and cold heat exchanger side separately. The relative differences between experimental and corrected overall thermal resistances were in the range of ±5%.

The first version of the new statistical method, developed for the thermal characteristics determination, was introduced in [19] for the minichannel heat exchanger, but without consideration of the manifolds. Unlike in the previous study, the statistical method had to be completely redesigned to take the manifold heat transfer into account. However, the basic idea of the method is preserved: a statistical comparison of the experimental and corrected theoretical values to determine the correction coefficients and the use of the simultaneously varying fluid flow rates at both sides of the heat exchanger. In the presented new statistical method, the heat flow rates are used instead of thermal resistances in the first method [19].

This article presents a new statistical method for the determination of the preliminary thermal characteristics of a prototype minichannel heat exchanger. The thermal characteristic is presented as the total heat transfer rate of the heat exchanger. Experimental measurements were performed for single-phase laminar flows of distilled water in a counter-flow arrangement. The obtained volumetric flowrates are characterized by 12-fold variability, corresponding to the total range of Re = 117 ÷ 2 500. The considered heat exchanger has 9 parallel square channels of 2 × 2 mm cross-section and two rectangular inlet and outlet manifolds milled on both sides of a single aluminium plate. The heat exchanger has an unusual and specific design since the surface area of both manifolds represented about 30% of the total heat transfer surface area. It was predicted that this effect could disturb the thermal behaviour of the heat exchanger and could constitute a significant part of the total heat transfer rate, which was later confirmed. The consideration of the effect of heat transfer in manifold regions for detailed determination of thermal characteristics requires the development of a new method of statistical analysis of experimental measurement results. This new statistical method, based on the Wilson plot approach, enables the assessment of heat transfer in the manifolds region and in the channels region separately. The additional considered effect is heat loss to the ambient, which was found to be negligible afterwards. In order to determine the corrected heat transfer rates, both in the manifolds and channels area, the correction coefficients were obtained using the least squares method. Calculations for the channel region are more precise due to the determination of separate correction coefficients for hot and cold heat exchanger sides, while for the manifold region, one common correction coefficient is determined. The comparison of the experimental and statistically corrected heat transfer rates, expressed in the form of relative differences (residuals), is presented for 2 calculation variants. In the first variant, heat transfer in the manifolds is neglected. In the second variant, the manifolds are included. As a result, an increase in the coefficient of determination R^2 is observed for the second model, which proves the importance of consideration of the heat transfer in the manifolds in the thermal analysis of the investigated minichannel heat exchanger.

2. Description of the experimental investigation

The real view of the experimental test stand for heat exchangers investigations was depicted in Fig. 1 and a detailed characterization of the design, specification of measurement procedure as well as calibration process was presented in [20].

Fig. 1. The picture of the experimental setup: 1 – calibration bath of the cold side, 2 – calibration bath of the hot side, 3 – hot and cold side pressure transducers, 4 – ice point reference, 5 – LabVIEW control program, 6 – Keithley digital multimeter, 7 – investigated minichannel heat exchanger with insulation, 9 – hot and cold side flow meters.

The experimental facility, which operates in a closed loop of circulating hot and cold working fluid, consisted of the investigated minichannel heat exchanger placed in the insulation, the thermocouples, pressure transducers, flowmeters, calibration baths and the measuring control unit. As a reference temperature, the automatic Ice Point Reference unit was used. The entire data registration and acquisition process, as well as the general operation of the test stand, were performed automatically. The Keithley measuring set was used to register the experimental data points and for its further processing, the LabVIEW environment was implemented. The proper measurements have been carried out in steady-state thermal conditions. The following parameters were directly measured: the inlet and outlet fluid temperatures, pressure drops and volumetric flowrates. On the basis of the registered parameters, the thermal power of investigated heat exchanger is obtained with the use of thermal balance method.

The view of investigated minichannel plate with selected manifold pairs is presented in Fig. 2a. The external dimensions of investigated heat exchanger are equal to 150 × 70 mm. The heat exchanger of a modular construction and sandwich form consists of the replaceable aluminum plate with minichannels placed between upper and bottom housing made from plastic. Rubber seals are also inserted on both sides between the aluminum plate and housings. The set of straight, parallel, square-shaped minichannels is milled on both sides of the single aluminum plate, forming symmetric grooves. The channel hydraulic diameter was equal to 2 mm. The plate has its own inlet and outlet manifolds milled on both sides of the plate as well. The working fluids flow through the same core material, therefore a prototype single-plate minichannel heat exchanger is constructed. The detailed geometry specification of channels and manifolds of the tested heat exchanger is shown in Fig. 2b. The main benefit of this solution is a simplified design with no intermediate plates inside, the reduced amount of heat exchanger components and rapid manufacturing. However, as far as the thermal design of this minichannel configuration is concerned, the channel top surfaces are thermally isolated due to the presence of rubber seals. It follows that only 3 inner sides of a square channel are heated or cooled, thus for accurate description of thermal characteristics of this particular minichannel system, the proper calculation variant for the Nusselt number should be selected. The thickness of the plate layer (intermediate wall),

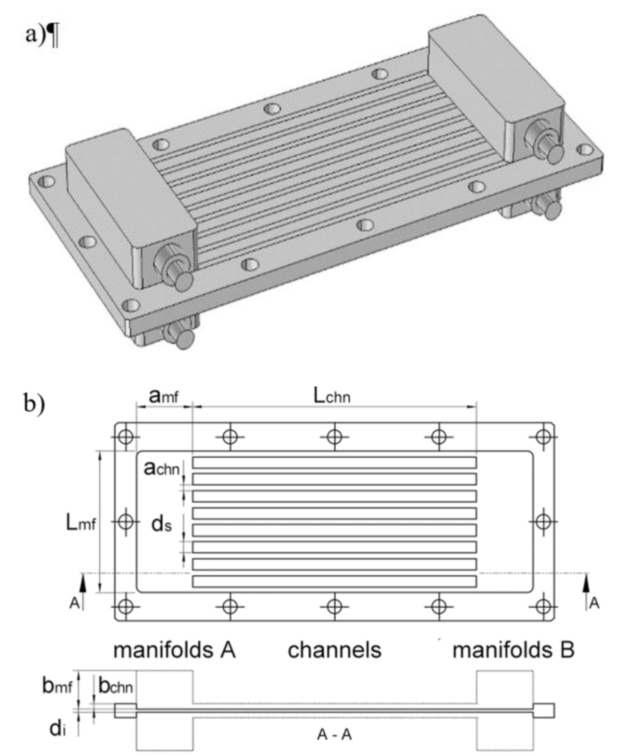

Fig. 2. Schematic view of the minichannel's plate with two pairs of manifolds (a), and sizes of the minichannels and manifolds (b).

which separates the hot and cold fluid is equal to 1 mm. Inlet and outlet plenum has a rectangular shape and both surface area occupy about 30% of the total heat transfer area. The heat exchanger is placed in the thermal insulation made of granulated polystyrene foam.

The experimental measurements were performed for single-phase flows of distilled water in a counterflow arrangement. The only parameter which was varied during measurements was the water flowrate. The inlet temperatures of hot and cold fluids were invariant and adjusted to 70°C and 20°C, respectively. A total of 8 series of measurements with significant variability of the volumetric flowrates were performed. In each series, the flowrate of the cold fluid was adjusted manually, while the flowrate of the hot fluid was maintained constant. Also, the flowrate was reduced from its maximum value (about 1.11 dm^3/min for cold fluid and 1.16 dm^3/min for hot fluid) by approximately 0.15 dm^3/min. Therefore, 8 measurement points were obtained in each series, and the total amount of $N = 64$ measurements were carried out. Due to low flow rates, laminar flows took place.

The thorough determination of experimental measurements uncertainty of individual parameters was presented in [20] and obtained results were collected in Table 1.

Table 1. Results of experimental measurements uncertainty determination.

Measurement	Uncertainty
Pressure	±0.05% of measurement range
Flow rate	±0.35% of measured value
Temperature	±0.25°C

The heat exchanger's dimensions, shown in Fig. 2b, are as follows: channel length $L_{chn} = 100$ mm, channel width $a_{chn} = 2$ mm, channel height $b_{chn} = 2$ mm (aspect ratio 1), manifold length $L_{mf} = 50$ mm, manifold width $a_{mf} = 20$ mm, manifold height $b_{mf} = 14$ mm, intermediate wall thickness $d_i = 1$ mm, side wall thickness $d_s = 4$ mm. The number of channels is $n_{chn} = 9$.

3. Statistical analysis of the measurement data and derivation of the thermal characteristics

Heat flow rates at the hot and cold heat exchanger side are calculated from Eqs. (1) and (2):

$$\dot{Q}_h = \dot{m}_h \cdot \Delta h_h = \dot{m}_h \cdot \left[h\left(T_{h,in}, p_{h,in}\right) - h\left(T_{h,out}, p_{h,out}\right)\right], \tag{1}$$

$$\dot{Q}_c = \dot{m}_c \cdot \Delta h_c = \dot{m}_c \cdot \left[h\left(T_{c,out}, p_{c,out}\right) - h\left(T_{c,in}, p_{c,in}\right)\right], \tag{2}$$

where the mass flow rates are given by:

$$\dot{m}_h = \dot{V}_h \cdot \rho\left(T_{h,out}, p_{h,out}\right), \tag{3}$$

$$\dot{m}_c = \dot{V}_c \cdot \rho\left(T_{c,out}, p_{c,out}\right). \tag{4}$$

For calculation purposes arithmetic mean is used:

$$\dot{Q}_{exp,i} = \left(\dot{Q}_{h,i} + \dot{Q}_{c,i}\right)/2, \tag{5}$$

for $i = 1, 2, ..., N$.

In order to assess heat loss to the ambient, the relative deviation $\delta\dot{Q}_{rel}$ of $\dot{Q}_h$ and $\dot{Q}_c$, relative to $\dot{Q}_{exp}$, is calculated as an average of the half $\left|\dot{Q}_h - \dot{Q}_c\right|/2$ of the distance between $\dot{Q}_h$ and $\dot{Q}_c$ divided by the mean heat flow $\dot{Q}_{exp}$:

$$\delta\dot{Q}_{rel} = \frac{1}{2 \cdot N} \cdot \sum_{i=1}^{N} \frac{\left|\dot{Q}_{h,i} - \dot{Q}_{c,i}\right|}{\dot{Q}_{exp,i}}. \tag{6}$$

It is more pessimistic than the standard deviation.

Due to the sufficient thermal insulation, the relative scattering of $\dot{Q}_{exp}$ amounted only $\pm\delta\dot{Q}_{rel} = \pm 3.1\%$ and therefore heat transfer to the ambient could be acknowledged as negligible.

Figure 3 presents the thermal balance of the heat exchanger in the form of experimentally obtained heat transfer rates of the cold and hot side.

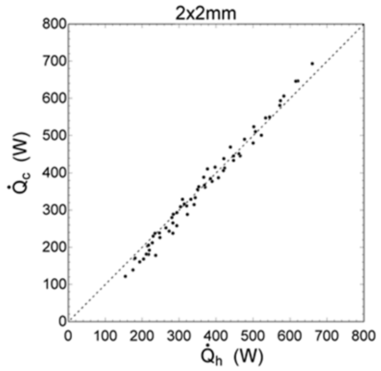

Fig. 3. Experimental heat transfer rates of the hot and cold side of the investigated heat exchanger.

In the developed statistical method the greatest possible variability of both flow rates, $\dot{V}_h$, $\dot{V}_c$ is required.

The Reynolds number Re_h, Re_c in each hot and cold channel or manifold is given by:

$$\mathrm{Re} = \frac{\dot{m}/S \cdot d_h}{\mu}. \tag{7}$$

The fluid's dynamic viscosity μ (and the thermal conductivity λ and the specific heat capacity c_p) in the channels is determined for the mean temperature between the inlet and outlet and in the manifolds for the corresponding inlet or outlet temperature. The hydraulic diameter is calculated from the same formula for the manifolds and channels:

$$d_h = \frac{2 \cdot a \cdot b}{a+b}. \tag{8}$$

The total cross-sectional area S is calculated by:

– for the manifolds:

$$S = a_{mf} \cdot b_{mf}, \tag{9}$$

– for the channels:

$$S = n_{chn} \cdot a_{chn} \cdot b_{chn}. \tag{10}$$

Figures 4a and 4b show the maps of the experimentally obtained volumetric flowrates and of the corresponding Reynolds number, respectively. The numbers show the order of measurements.

In the statistical method developed in this paper, the significant heat transfer area of the manifolds is taken into account. To present the significance of the heat transfer in the manifolds, two variants of the calculation are developed: with the neglected manifolds and with the manifolds taken into account. Figure 5 depicts these two variants of the heat flows.

The manifolds are partly made of metal and plastic, schematically shown in Fig. 2. The heat transfer area in the single pair of manifolds is given by:

$$A_{mf} = L_{mf} \cdot a_{mf} + 2 \cdot (L_{mf} + a_{mf}) \cdot b_{chn}. \tag{11}$$

The heat transfer area of n_{chn} channels, with only 3 sides exchanging heat, is given by:

$$A_{chn} = n_{chn} \cdot L_{chn} \cdot (a_{chn} + 2 \cdot b_{chn}). \tag{12}$$

Substitution of the numerical values gives $A_{mf} = 0.00128$ m^2 and $A_{chn} = 0.00540$ m^2. Both manifold's heat transfer area is equal to $2A_{mf}/(2A_{mf}+A_{chn}) \approx 32.2\%$ of the total heat transfer area.

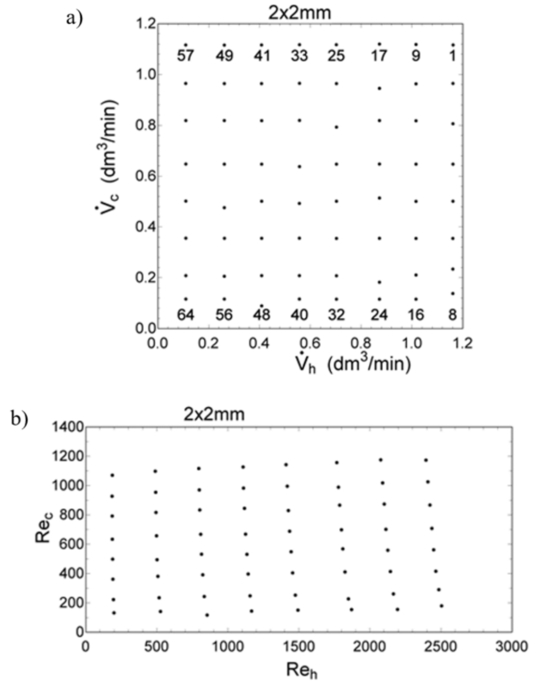

Fig. 4. Maps of the experimental: a) volumetric flowrates with the order of measurements, and b) corresponding Reynolds numbers.

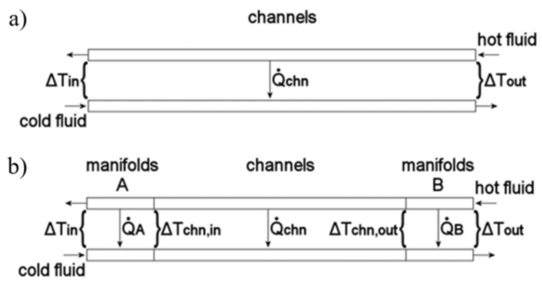

Fig. 5. Heat flows in two variants: a) without manifolds, b) with manifolds.

The theoretical (predicted) values of the heat transfer coefficient α are calculated from the appropriate correlations of the Nusselt number:

$$\alpha_{pred} = \frac{\mathrm{Nu}_{pred} \cdot \lambda}{d_h}. \tag{13}$$

In the manifolds the Nusselt number in this paper is calculated from the Dittus-Boelter correlation [21]:

$$\mathrm{Nu}_{pred} = 0.023 \cdot \mathrm{Re}^{0.8} \cdot \mathrm{Pr}^{0.4}, \tag{14}$$

where the Prandtl number is given by:

$$\mathrm{Pr} = \frac{c_p \cdot \mu}{\lambda}. \tag{15}$$

Although the flows in the manifolds are three dimensional, they are turbulent and the Dittus-Boelter correlation, developed for the flows in pipes, is used as a rough approximation.

In the channels, the way the Nusselt number is calculated depends on the flow type.

For developing laminar flows (Re < 2 300) in a rectangular microchannel the Nusselt number is given by the formula from [22], used for the normalized aspect ratio $0.1 \le r_{ba} \le 1$:

$$\mathrm{Nu}_{pred} = \frac{1}{C_1 \cdot (L^*)^{C_2 + C_3}} + C_4. \tag{16}$$

The dimensionless thermal channel's length L^* and the coefficients $C_1, \dots, C_4$ are given by:

$$L^* = \frac{L/d_h}{\mathrm{Re} \cdot \mathrm{Pr}}, \tag{17}$$

$$C_1 = -2.757 \cdot \frac{10^{-3}}{r_{ba}^3} + 3.274 \cdot \frac{10^{-2}}{r_{ba}^2} - 7.464 \cdot \frac{10^{-5}}{r_{ba}} + 4.476, \tag{18}$$

$$C_2 = 0.6391, \tag{19}$$

$$C_3 = 1.604 \cdot \frac{10^{-4}}{r_{ba}^2} - 2.622 \cdot \frac{10^{-3}}{r_{ba}} + 2.568 \cdot 10^{-2}, \tag{20}$$

$$C_4 = -6.094 \cdot r_{ba}^3 + 15.19 \cdot r_{ba}^2 - 13.11 \cdot r_{ba} + 7.301, \tag{21}$$

where the normalized aspect ratio is given by:

$$r_{\mathrm{ba}} = \min(a_{chn}/b_{chn}; b_{chn}/a_{chn}). \tag{22}$$

For $L^* < 0.1$, laminar flows are developed [23].

For fully developed laminar flow, the Nusselt number is given by [24]:

$$\mathrm{Nu}_{fd,pred} = 8.235 \cdot (1 - 2.0421 r_{ba} + 3.0853 r_{ba}^2 + -2.4765 r_{ba}^3 + 1.0578 r_{ba}^4 - 0.1861 r_{ba}^5). \tag{23}$$

The analytical formula for fully developed laminar flows is also derived in [25]. For transitional flows 2 300 < Re < 10 000 the linear interpolation from Gnielinski correlation [26,27] is used. It is based on the values of $\mathrm{Nu}_{lam,2300}$ for the laminar flow of Re = 2 300 (16) and $\mathrm{Nu}_{turb,10000}$ for the turbulent flow of Re = 10 000 (14):

$$\mathrm{Nu}_{pred} = \left(1 - \frac{\mathrm{Re} - 2300}{10000 - 2300}\right) \cdot \mathrm{Nu}_{lam,2300} + + \frac{\mathrm{Re} - 2300}{10000 - 2300} \cdot \mathrm{Nu}_{turb,10000}. \tag{24}$$

For turbulent flows Re > 10 000 the Dittus-Boelter formula (14) is used.

In the investigated heat exchanger only 3 from 4 channels sides are heated or cooled. In this case the approximate formula from [23] is used to calculate the Nusselt number for 3 sides only:

$$\mathrm{Nu}_{pred} = \mathrm{Nu}_{4,pred} \cdot \frac{\mathrm{Nu}_{fd,3}}{\mathrm{Nu}_{fd,4}}, \tag{25}$$

where $\mathrm{Nu}_{4,pred}$ is given by the formulae (14), (16) or (24) in which the subscript 4 is omitted for simplicity. The quotient $\mathrm{Nu}_{fd,3}/\mathrm{Nu}_{fd,4}$ is calculated based on the values of $\mathrm{Nu}_{fd,3}$ and $\mathrm{Nu}_{fd,4}$ for the fully developed flows [24] and is presented in Table 2 for various aspect ratios a/b.

Table 2. Quotients $\mathrm{Nu}_{fd,3}/\mathrm{Nu}_{fd,4}$ for various values of the aspect ratio a/b.

Aspect ratio a/b	$\mathrm{Nu}_{fd,3}$	$\mathrm{Nu}_{fd,4}$	$\mathrm{Nu}_{fd,3}/\mathrm{Nu}_{fd,4}$
0	8.235	8.235	1
0.1	6.939	6.7	1.03567
0.2	6.072	5.704	1.06452
0.3	5.393	4.969	1.08533
0.4	4.885	4.457	1.09603
0.5	4.505	4.111	1.09584
0.7	3.991	3.74	1.06711
1.0	3.556	3.599	0.98805
1.43	3.195	3.74	0.85428
2.0	3.146	4.111	0.76526
2.5	3.169	4.457	0.71102
3.33	3.306	4.969	0.66533
5	3.636	5.704	0.63745
10	4.252	6.7	0.63463
∞	5.385	8.235	0.65392

In the analyzed heat exchanger, three heat flows take place: $\dot{Q}_{\mathrm{A}}$ in the pair of manifolds A, $\dot{Q}_{chn}$ in the channels and $\dot{Q}_{\mathrm{B}}$ in the pair of manifolds B. The predicted values of these flows are calculated from the above-described formulae for the Nusselt number. However, these predicted heat flows should be multiplied by the correction coefficients and the obtained corrected heat flows are statistically compared with the experimental ones. The statistical method of least squares is used to determine these correction coefficients.

Theoretical, predicted heat transfer coefficients are calculated from appropriate Nusselt number correlations. In the manifold pairs the Dittus-Boelter correlation is used and in the channels the correlation (16) in [22] is applied, regarding thermally developing flows in rectangular channels. The corrected overall heat transfer coefficients in two pairs of manifolds and in the channels are calculated using the statistically determined correction coefficients c_h, c_c, c_{AB}, which correct the theoretically predicted heat transfer coefficients:

$$k_{\mathrm{A},corr} = c_{\mathrm{AB}} \cdot k_{\mathrm{A},pred}, \tag{26}$$

$$\frac{1}{k_{chn,corr}} = \frac{1}{c_h \cdot \alpha_{h,chn,pred}} + \frac{1}{c_c \cdot \alpha_{c,chn,pred}}, \tag{27}$$

$$k_{\mathrm{B},corr} = c_{\mathrm{AB}} \cdot k_{\mathrm{B},pred}. \tag{28}$$

The predicted overall heat transfer coefficients $k_{\mathrm{A},pred}$ and $k_{\mathrm{B},pred}$ in the manifolds pairs A and B are calculated using the heat transfer coefficients $\alpha_{h,\mathrm{A},pred}$, $\alpha_{c,\mathrm{A},pred}$, $\alpha_{h,\mathrm{B},pred}$, $\alpha_{c,\mathrm{B},pred}$ from the Dittus-Boelter correlation (14):

$$\frac{1}{k_{\mathrm{A},pred}} = \frac{1}{\alpha_{h,\mathrm{A},pred}} + \frac{1}{\alpha_{c,\mathrm{A},pred}}, \tag{29}$$

$$\frac{1}{k_{\mathrm{B},pred}} = \frac{1}{\alpha_{h,\mathrm{B},pred}} + \frac{1}{\alpha_{c,\mathrm{B},pred}}. \quad (30)$$

Because the main heat flow takes place between hot and cold channels, two separate correction coefficients c_h, c_c are used. For both pairs of manifolds, only one common correction coefficient, c_{AB}, is used. Since there is relatively small number N of the measurements, it is better to statistically determine maximum 3 correction coefficients [19].

The temperature differences of the hot and cold working fluid in the region borders are related by following equations:

$$\Delta T_{chn,in} = \Delta T_{in} \cdot \exp\left(\frac{k_{\mathrm{A}corr} \cdot A_{\mathrm{A}}}{W_{\mathrm{A}}}\right), \quad (31)$$

$$\Delta T_{chn,out} = \Delta T_{chn,in} \cdot \exp\left(\frac{k_{chncorr} \cdot A_{chn}}{W_{chn}}\right), \quad (32)$$

$$\Delta T_{out} = \Delta T_{chn,out} \cdot \exp\left(\frac{k_{\mathrm{B}corr} \cdot A_{\mathrm{B}}}{W_{\mathrm{B}}}\right), \quad (33)$$

where the resultant heat capacity rates for the counter-current flows:

$$\frac{1}{W_{\mathrm{A}}} = \frac{1}{\dot{m}_h \cdot c_{p,\mathrm{A},h}} - \frac{1}{\dot{m}_c \cdot c_{p,\mathrm{A},c}}, \quad (34)$$

$$\frac{1}{W_{chn}} = \frac{1}{\dot{m}_h \cdot c_{p,chn,h}} - \frac{1}{\dot{m}_c \cdot c_{p,chn,c}}, \quad (35)$$

$$\frac{1}{W_{\mathrm{B}}} = \frac{1}{\dot{m}_h \cdot c_{p,\mathrm{B},h}} - \frac{1}{\dot{m}_c \cdot c_{p,\mathrm{B},c}}. \quad (36)$$

The statistically corrected heat transfer rates in the channels and manifolds are described by:

$$\dot{Q}_{\mathrm{A},corr} = k_{\mathrm{A},corr} \cdot A_{\mathrm{A}} \cdot \Delta T_{log,\mathrm{A}}, \quad (37)$$

$$\dot{Q}_{chn,corr} = k_{chn,corr} \cdot A_{chn} \cdot \Delta T_{log,chn}, \quad (38)$$

$$\dot{Q}_{\mathrm{B},corr} = k_{\mathrm{B},corr} \cdot A_{\mathrm{B}} \cdot \Delta T_{log,\mathrm{B}}, \quad (39)$$

where the logarithmic mean temperature differences in the channels and two pairs of manifolds are given by:

$$\Delta T_{log,\mathrm{A}} = \frac{\Delta T_{chn,in} - \Delta T_{in}}{\ln\frac{\Delta T_{chn,in}}{\Delta T_{in}}}, \quad (40)$$

$$\Delta T_{log,chn} = \frac{\Delta T_{chn,out} - \Delta T_{chn,in}}{\ln\frac{\Delta T_{chn,out}}{\Delta T_{chn,in}}}, \quad (41)$$

$$\Delta T_{log,\mathrm{B}} = \frac{\Delta T_{out} - \Delta T_{chn,out}}{\ln\frac{\Delta T_{out}}{\Delta T_{chn,out}}}. \quad (42)$$

The overall and statistically corrected heat transfer rate is a sum of three heat flows:

$$\dot{Q}_{corr} = \dot{Q}_{\mathrm{A},corr} + \dot{Q}_{chn,corr} + \dot{Q}_{\mathrm{B},corr}. \quad (43)$$

This concise formula (43) presents the thermal characteristic of the investigated heat exchanger, in which the right side depends on the flow rates $\dot{V}_h$, $\dot{V}_c$ and contains the statistically determined correction coefficients c_h, c_c, c_{AB}. The first calculation variant (without manifolds) is obtained by the substitution $c_{\mathrm{AB}} = 0$, which indicates that no heat transfer in the manifold region occurs ($\dot{Q}_{\mathrm{A},corr} = \dot{Q}_{\mathrm{B},corr} = 0$).

The correction coefficients c_h, c_c, c_{AB} are determined by statistical fitting the corrected $\dot{Q}_{chn,corr}$ and experimental $\dot{Q}_{chn,exp}$ heat flows in the channels, by the method of least squares.

The corrected heat flow in the channels may be presented with explicitly shown the correction coefficients c_h, c_c:

$$\dot{Q}_{chn,corr} = \left(\frac{1}{c_h \cdot \alpha_{h,chn,pred}} + \frac{1}{c_c \cdot \alpha_{c,chn,pred}}\right)^{-1} \cdot A_{chn} \cdot \Delta T_{log,chn}. \quad (44)$$

The experimental heat flow in the channels $\dot{Q}_{chn,exp}$ is not measured directly, however it is approximated by subtracting the corrected heat transfer rates in the pair of manifold A and B from the measured total heat flow $\dot{Q}_{exp}$:

$$\dot{Q}_{chn,exp} = \dot{Q}_{exp} - \dot{Q}_{\mathrm{A},corr} - \dot{Q}_{\mathrm{B},corr}, \quad (45)$$

or in the form with explicitly shown the correction coefficient c_{AB}:

$$\dot{Q}_{chn,exp} = \dot{Q}_{exp} - c_{\mathrm{AB}} \cdot k_{\mathrm{A},pred} \cdot A_{\mathrm{A}} \cdot \Delta T_{log,\mathrm{A}} - c_{\mathrm{AB}} \cdot k_{\mathrm{B},pred} \cdot A_{\mathrm{B}} \cdot \Delta T_{log,\mathrm{B}}. \quad (46)$$

It is easier to statistically fit the reciprocals $\dot{Q}_{chn,corr}^{-1}$ and $\dot{Q}_{chn,exp}^{-1}$ because the correction coefficients c_h, c_c are determined analytically in this case. The reciprocal $\dot{Q}_{chn,corr}^{-1}$ (44) is written as:

$$\dot{Q}_{chn,corr}^{-1} = \left(\frac{1}{c_h \cdot \alpha_{h,chn,pred}} + \frac{1}{c_c \cdot \alpha_{c,chn,pred}}\right) \cdot \frac{1}{A_{chn} \cdot \Delta T_{log,chn}}, \quad (47)$$

or in the version where the $1/c_h$ and $1/c_c$ are in a linear form:

$$\dot{Q}_{chn,corr}^{-1} = \frac{1}{c_h} \cdot \frac{1}{\alpha_{h,chn,pred} \cdot A_{chn} \cdot \Delta T_{log,chn}} + \frac{1}{c_c} \cdot \frac{1}{\alpha_{c,chn,pred} \cdot A_{chn} \cdot \Delta T_{log,chn}}. \quad (48)$$

The reciprocal of experimental heat transfer rates in the channels is given by:

$$\dot{Q}_{chn,exp}^{-1} = (\dot{Q}_{exp} - c_{\mathrm{AB}} \cdot k_{\mathrm{A},pred} \cdot A_{\mathrm{A}} \cdot \Delta T_{log,\mathrm{A}} - c_{\mathrm{AB}} \cdot k_{\mathrm{B},pred} \cdot A_{\mathrm{B}} \cdot \Delta T_{log,\mathrm{B}})^{-1}. \quad (49)$$

The correction coefficients c_h, c_c, c_{AB} are determined statistically by the use of the least square method [28] by minimizing the sum:

$$\varphi(c_h, c_c, c_{\mathrm{AB}}) = \sum_{i=1}^{N}\left[\dot{Q}_{chn,exp,i}^{-1}(c_{\mathrm{AB}}) - \dot{Q}_{chn,corr,i}^{-1}(c_h, c_c)\right]^2. \quad (50)$$

The short symbols are used for the convenience:

$$y = \dot{Q}_{chn,exp}^{-1}, \qquad x_h = 1/\left(\alpha_{h,chn,pred} \cdot A_{chn} \cdot \Delta T_{log,chn}\right),$$

$$x_c = 1/\left(\alpha_{c,chn,pred} \cdot A_{chn} \cdot \Delta T_{log,chn}\right),$$

$$a_h = 1/c_h, \qquad a_c = 1/c_c.$$

Using these symbols, the reciprocal $\dot{Q}^{-1}_{chn,corr}$ in Eq. (48) has the clear form of a linear function of two variables x_h, x_c:

$$\dot{Q}^{-1}_{chn,corr} = a_h \cdot x_h + a_c \cdot x_c. \tag{51}$$

Minimization of the function (50) for c_h, c_c gives the linear system of equation with two unknowns a_h, a_c, similar to the system in [19]:

$$\begin{cases} a_h \cdot \sum_{i=1}^{N} x_{h,i}^2 & +a_c \cdot \sum_{i=1}^{N} x_{h,i} x_{c,i} & = \sum_{i=1}^{N} x_{h,i} y_i \\ a_h \cdot \sum_{i=1}^{N} x_{h,i} x_{c,i} & +a_c \cdot \sum_{i=1}^{N} x_{c,i}^2 & = \sum_{i=1}^{N} x_{c,i} y_i \end{cases}. \tag{52}$$

The linear coefficients a_h, a_c are calculated analytically by the use of the Cramer's rule:

$$a_h = \frac{\sum_{i=1}^{N} x_{c,i}^2 \cdot \sum_{i=1}^{N} x_{h,i} y_i - \sum_{i=1}^{N} x_{h,i} x_{c,i} \cdot \sum_{i=1}^{N} x_{c,i} y_i}{\sum_{i=1}^{N} x_{h,i}^2 \cdot \sum_{i=1}^{N} x_{c,i}^2 - \left(\sum_{i=1}^{N} x_{h,i} x_{c,i}\right)^2}, \tag{53}$$

$$a_c = \frac{\sum_{i=1}^{N} x_{h,i}^2 \cdot \sum_{i=1}^{N} x_{c,i} y_i - \sum_{i=1}^{N} x_{h,i} x_{c,i} \cdot \sum_{i=1}^{N} x_{h,i} y_i}{\sum_{i=1}^{N} x_{h,i}^2 \cdot \sum_{i=1}^{N} x_{c,i}^2 - \left(\sum_{i=1}^{N} x_{h,i} x_{c,i}\right)^2}. \tag{54}$$

The correction coefficients c_h, c_c are calculated from:

$$c_h = \frac{1}{a_h}, \qquad c_c = \frac{1}{a_c}. \tag{55}$$

The correction coefficient c_{AB} is calculated numerically, the Golden Section method is used to find the minimum of the function (50) for c_{AB}. In every iteration of this method the coefficients c_h, c_c are calculated analytically from (55). This decomposition of the calculation into the linear and nonlinear part reduces the calculation time and gives better accuracy of the values of the coefficients c_h, c_c, c_{AB}.

The coefficient of determination is given by [28]:

$$R^2 = 1 - \frac{\sum_{i=1}^{N} \left(\dot{Q}_{exp,i} - \dot{Q}_{corr,i}\right)^2}{\sum_{i=1}^{N} \left(\dot{Q}_{exp,i} - 1/N \cdot \sum_{j=1}^{N} \dot{Q}_{exp,j}\right)^2}. \tag{56}$$

The relative residuals between the experimental and statistically corrected heat flow in the heat exchanger are calculated as:

$$res_{rel,i} = \frac{\dot{Q}_{exp,i} - \dot{Q}_{corr,i}}{\dot{Q}_{corr,i}}, \tag{57}$$

for $i = 1, 2, ..., N$.

The computer program was developed in the Engineering Equation Solver (EES) environment to calculate the results.

Figure 6 presents the relative residuals of the experimental and statistically corrected heat transfer rates for the heat exchanger, compiled for two calculation models. Figure 6a corresponds to the model, where the heat transfer in the manifolds was neglected (0-mf symbol), while Fig. 6b denotes the model, where the heat transfer in the manifolds is included.

Each measurement was done after 20–25 minutes of the temperatures stabilization, to reach the steady state, which means the measurements are statistically independent. However there are regularities in Fig. 6, but they are caused by the regular changes of the flowrates, measured in the order shown in Fig. 4a. The regularities also exist in Fig. 6b, where the heat flows in the manifolds are taken into account, but the residuals are significantly lower and are more random.

The highest residuals occur in the primary measurements, what corresponds to the highest flow rates and Reynolds numbers, Fig. 4a. The residuals in Fig. 6b are much lower than in Fig. 6a, which means that the consideration of heat flows in the manifolds is important. Calculation results of the correction coefficients and the coefficients of determination R^2 are presented in Table 3.

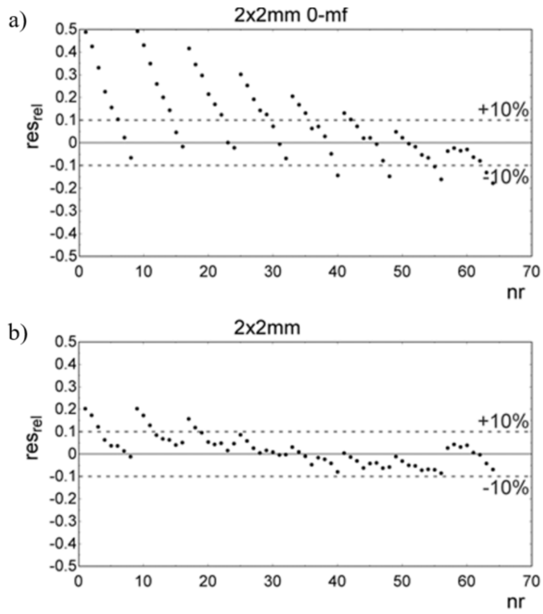

Fig. 6. Relative residuals of the experimental and statistically corrected heat transfer rates in the heat exchanger. Variants: a) without manifolds (0-mf), b) with manifolds.

Table 3. Calculation results for the variants 1 and 2.

Variant	c_{AB}	c_h	c_c	R^2
1 – without manifolds (0-mf)	0	1.529	2.009	0.8827
2 – with manifolds	7.751	1.081	1.549	0.9335

The statistically determined correction coefficients c_{AB}, c_h, c_c in the variant 2 are used in the heat exchanger's thermal characteristics (43).

4. Conclusions

- The use of the proper thermal insulation enables neglecting the heat transfer to the ambient. The experimental difference of ±3.1% between the heat flow supplied and removed from the heat exchanger is slight and therefore the heat flow to the environment may be omitted.
- The statistical method for the determination of preliminary thermal characteristic of minichannel heat exchangers with significant manifolds dimensions was developed.
- The consideration of significant heat transfer in the manifold region improves the fit accuracy (coefficient of determination R^2) with respect to the model, where mani-

folds were not considered. The relative differences between the experimental and statistically corrected heat flows are much decreased.

- In order to describe precisely thermal behavior of investigated minichannel heat exchanger and to obtain exact thermal characteristics, further extended analysis is required.

References

[1] Rosa, P., Karayiannis, T.G., & Collins, M.W. (2009). Single-phase heat transfer in microchannels: The importance of scaling effects. *Applied Thermal Engineering*, 29(17–18), 3447–3468. doi: 10.1016/j.applthermaleng.2009.05.015

[2] Morini, G.L. (2004). Single-phase convective heat transfer in microchannels: A review of experimental results. *International Journal of Thermal Sciences*, 43(7), 631–651. doi: 10.1016/j.ijthermalsci.2004.01.003

[3] Hasan, M.I., Rageb, A.A., Yaghoubi, M., & Homayoni, H. (2009). Influence of channel geometry on the performance of a counter flow microchannel heat exchanger. *International Journal of Thermal Sciences*, 48(8), 1607–1618. doi: 10.1016/j.ijthermalsci.2009.01.004

[4] Steinke, M.E., & Kandlikar, S.G. (2005). Single-phase liquid heat transfer in microchannels. In *Proceedings of ICMM2005*, *ASME 3rd International Conference on Nanochannels*, *Microchannels, and* Minichannels, 41855, (pp. 667–678), 13−15 June, Toronto, Ontario, Canada. doi:10.1115/ICMM2005-75114

[5] Dixit, T., & Ghosh, I. (2015). Review of micro-and mini-channel heat sinks and heat exchangers for single phase fluids. *Renewable and Sustainable Energy Reviews*, 41, 1298–1311. doi: 10.1016/j.rser.2014.09.024

[6] Foli, K., Okabe, T., Olhofer, M., Jin, Y., & Sendhoff, B. (2006). Optimization of micro heat exchanger: CFD, analytical approach and multi-objective evolutionary algorithms. *International Journal of Heat and Mass Transfer*, 49(5–6), 1090–1099. doi: 10.1016/j.ijheatmasstransfer.2005.08.032

[7] Kee, R.J., Almand, B.B., Blasi, J.M., Rosen, B.L., Hartmann, M., Sullivan, N.P., & Martin, J.L. (2011). The design, fabrication, and evaluation of a ceramic counter-flow microchannel heat exchanger. *Applied Thermal Engineering*, 31(11–12), 2004–2012. doi: 10.1016/j.applthermaleng.2011.03.009

[8] García-Hernando, N., Acosta-Iborra, A., Ruiz-Rivas, U., & Izquierdo, M. (2009). Experimental investigation of fluid flow and heat transfer in a single-phase liquid flow micro-heat exchanger. *International Journal of Heat and Mass Transfer*, 52(23–24), 5433–5446. doi: 10.1016/j.ijheatmasstransfer.2009.06.034

[9] Cao, H., Chen, G., & Yuan, Q. (2009). Testing and design of a microchannel heat exchanger with multiple plates. *Industrial & Engineering Chemistry Research*, 48(9), 4535–4541. doi: 10.1021/ie801419r

[10] Koyama, K., & Asako, Y. (2010). Experimental investigation on heat transfer characteristics of a gas-to-gas counterflow microchannel heat exchanger. *Experimental Heat Transfer*, 23(2), 130−143. doi: 10.1080/08916150903402799

[11] Alm, B., Imke, U., Knitter, R., Schygulla, U., & Zimmermann, S. (2008). Testing and simulation of ceramic micro heat exchangers. *Chemical Engineering Journal*, 135, S179−S184. doi: 10.1016/j.cej.2007.07.005

[12] Al-Nimr, M.A., Maqableh, M., Khadrawi, A.F., & Ammourah, S.A. (2009). Fully developed thermal behaviors for parallel flow microchannel heat exchanger. *International Communications in Heat and Mass Transfer*, 36(4), 385−390. doi: 10.1016/j.icheatmasstransfer.2009.01.010

[13] Wajs, J., Mikielewicz, D., & Fornalik-Wajs, E. (2016). Thermal performance of a prototype plate heat exchanger with minichannels under boiling conditions. In *Proc. of 7th European Thermal-Sciences Conference (Eurotherm2016)*. *Journal of Physics: Conference Series*, 745(3), 032063. doi: 10.1088/1742-6596/745/3/032063

[14] Mikielewicz, D., & Wajs, J. (2017). Possibilities of heat transfer augmentation in heat exchangers with minichannels for marine applications. *Polish Maritime Research Special Issue*, 24, 133−140. doi: 10.1515/pomr-2017-0031

[15] Yang, Y., Brandner, J.J., & Morini, G.L. (2012). Hydraulic and thermal design of a gas microchannel heat exchanger. In *Journal of Physics: Conference Series*, 362(1), 012023. doi: 10.1088/1742-6596/362/1/012023

[16] Dang, T., Teng, J.T., & Chu, J C. (2010). A study on the simulation and experiment of a microchannel counter-flow heat exchanger. *Applied Thermal Engineering*, 30(14−15), 2163−2172. doi: 10.1016/j.applthermaleng.2010.05.029

[17] Tychanicz-Kwiecień, M. (2022). The application of the Wilson plot method to convective heat transfer-discussion. *Advances in Mechanical and Materials Engineering*, 39(94), 77−89. doi: 10.7862/rm.2022.6

[18] Fernando, P., Palm, B., Ameel, T., Lundqvist, P., & Granryd, E. (2008). A minichannel aluminium tube heat exchanger– Part I: Evaluation of single-phase heat transfer coefficients by the Wilson plot method. *International Journal of Refrigeration*, 31(4), 669−680. doi: 10.1016/j.ijrefrig.2008.02.011

[19] Rybiński, W., & Mikielewicz, J. (2018). Statistical method for the determination of the minichannel heat exchanger's thermal characteristics. *Energy*, 158, 139−147. doi: 10.1016/j.energy.2018.05.175

[20] Tychanicz-Kwiecień, M., Smusz, R., & Gil, P. (2019). The design of experimental set-up for testing of heat exchangers. In *Contemporary issues of heat and mass transfer*, 2 (pp. 901−918). Publishing House of the Koszalin University of Technology.

[21] Mobedi, M., & Gediz Illis G. (2023). *Fundamentals of Heat Transfer: An Interdisciplinary Analytical Approach*. Springer Nature Singapore. doi:10.1007/978-981-99-0957-5

[22] Lee, P.S., & Garimella, S.V. (2006). Thermally developing flow and heat transfer in rectangular microchannels of different aspect ratios. *International Journal of Heat and Mass Transfer*, 49, 3060−3067. doi: 10.1016/j.ijheatmasstransfer.2006.02.011

[23] Kandlikar, S.G., Garimella, S., Li, D., Colin, S., & King, M.R. (2006). *Heat transfer and fluid flow in minichannels and microchannels*. Elsevier Ltd., Oxford.

[24] Shah, R.K., & London, A.L. (1978). *Laminar flow forced convection in ducts*. Academic Press, New York.

[25] Rybiński, W., & Mikielewicz, J. (2014). Analytical solutions of heat transfer for laminar flow in rectangular channels. *Archives of Thermodynamics*, 35(4), 29−42. doi: 10.2478/aoter-2014-0031

[26] Morini, G.L., Lorenzini, M., Salvigni, S., & Celata, G.P. (2010). Experimental analysis of microconvective heat transfer in the laminar and transitional regions. *Experimental Heat Transfer*, 23, 73−93. doi: 10.1080/08916150903402757

[27] Wilk, J. (2013). *Investigation of heat transfer in short minichannels*. Publishing House of the Rzeszów University of Technology.

[28] Brandt, S. (2014). *Data analysis. Statistical and computational methods for scientists and engineers* (4th Edn.). Springer.